

Catastrophic Phase Transitions and Early Warnings in a Spatial Ecological Model

A Fernández^{1‡} and H Fort^{2§}

¹Instituto de Física, Facultad de Ingeniería, Universidad de la República, Julio Herrera y Reissig 565, 11300 Montevideo, Uruguay.

²Instituto de Física, Facultad de Ciencias, Universidad de la República, Iguá 4225, 11400 Montevideo, Uruguay

Abstract. Gradual changes in exploitation, nutrient loading, etc. produce shifts between alternative stable states (ASS) in ecosystems which, quite often, are not smooth but abrupt or catastrophic. Early warnings of such catastrophic regime shifts are fundamental for designing management protocols for ecosystems. Here we study the spatial version of a popular ecological model, involving a logistically growing single species subject to exploitation, which is known to exhibit ASS. Spatial heterogeneity is introduced by a carrying capacity parameter varying from cell to cell in a regular lattice. Transport of biomass among cells is included in the form of diffusion. We investigate whether different quantities from statistical mechanics -like the variance, the two-point correlation function and the patchiness- may serve as early warnings of catastrophic phase transitions between the ASS. In particular, we find that the patch-size distribution follows a power law when the system is close to the catastrophic transition. We also provide links between spatial and temporal indicators and analyze how the interplay between diffusion and spatial heterogeneity may affect the earliness of each of the observables. We find that possible remedial procedures, which can be followed after these early signals, are more effective as the diffusion becomes lower. Finally, we comment on similarities and differences between these catastrophic shifts and paradigmatic thermodynamic phase transitions like the liquid-vapour change of state for a fluid like water.

‡ arielfer@fing.edu.uy

§ hugo@fisica.edu.uy

1. Introduction

Ecosystems are exposed to gradual change in external conditions such as climate, inputs of nutrients, toxic chemicals, etc. Although it is generally assumed that these gradual variations produce also gradual changes in the ecosystems, occasionally sudden catastrophic regime shifts may occur. Recent examples of ecosystems illustrating such changes are the shift in Caribbean coral reefs [1, 2], shallow lakes that become overgrown by floating plants [3], savannahs that are encroached suddenly by bushes [4, 5] and lakes that shift from clear to turbid [6, 7]. A simple explanation for such drastic shifts is that the ecosystem has alternative stable states (ASS) [8, 9]. In other words, under the same external conditions the system can be in two or more stable states. Hence, when subjected to a slowly changing external factor (such as climate), an ecosystem may show little change until it reaches a critical point where a sudden shift to an alternative contrasting state occurs. The presence of ASS implies that if a system has gone through such a state shift, it tends to remain in the new state until the control variable is changed back to a much lower level. This hysteresis phenomenon of "history dependent" alternative equilibrium states is well known in physics.

The simplest models for describing alternative states in ecosystems correspond to what are known in physics parlance as *mean-field* (MF) models. Neglecting all spatial heterogeneities, these models describe the change over time of some population that characterizes the state of the ecosystem. These models are easy to analyze and in cases without significant heterogeneity their predictions are not very different from those of spatial models. However, in other cases the presence of a spatial dimension profoundly alter population dynamics or opportunities for coexistence in the real world [10]. In fact, the oversimplification of MF models casts doubt on whether the occurrence of an alternative stable state could be an artifact. Moreover, verifications and predictive power with respect to catastrophic responses to changing environmental conditions are still scarce for spatially extensive ecosystems. Analysis of spatially explicit models are relevant for other reasons. For example, to understand phenomena like clumping and spatial segregation in plant communities [11]. It was shown that vegetation patches, which have been extensively studied for arid lands [12], can be approached as a pattern formation phenomenon [13]-[14]. It has been hypothesized that vegetation patchiness could be used as a signature of imminent catastrophic shifts between alternative states [15]. Evidences that the patch-size distribution of vegetation follows a power law were later found in arid Mediterranean ecosystems [16]. This implies that vegetation patches were present over a wide range of size scales, thus displaying scale invariance. It was also found that with increasing grazing pressure, the field data revealed deviations from power laws. Hence, the authors proposed that this power law behaviour may be a warning signal for the onset of desertification. These spatial *early warnings* complement temporal ones like the variance of time series introduced to detect lake eutrophication || [17] or the impact of pollutants [18].

In this work we will consider the spatial version of a general ecological model in terms of a logistically growing species whose consumption, loss or removal (either by grazing, predation or harvesting) is represented by a saturation curve [19, 20]. The MF version of this model, in terms of two parameters, is known to have ASS. In order to take into account the spatial heterogeneity of the landscape one of the two

|| Eutrophication is an increase in nutrients leading to an enhanced growth of aquatic vegetation or phytoplankton and further effects including lack of oxygen and severe reductions in water quality, fish, and other animal populations.

parameters, the *local* parameter, is taken as dependent on the position. The other parameter, the *global* or *control* parameter, is taken uniform in all the system. Our goal is to use this framework to analyze the following questions:

- (i) How spatial heterogeneity of the environment and diffusion of matter and organisms affect the existence of alternative stable states.
- (ii) Whether emergent characteristic spatial patterns are really useful as early warnings and how they are connected with temporal signs of catastrophic shifts.
- (iii) The search for scaling laws underlying spatial patterns and self-organization.

We will address these issues by measuring typical observables of statistical mechanics, like the spatial variance, the two-point correlation function and the patchiness.

This work is organized as follows. In section 2 we review the ecological MF model and analyze it from the point of view of Catastrophe Theory [21]. Section 3 is devoted to the methods used in this study and the characterization of the steady states reached by the system for static situations, *i.e.* constant values of the uniform parameter. In section 4 we study the dynamic case in which the uniform parameter is changing with time. This combination of a varying global control parameter, modelling a slowly changing stressor, and a local parameter, describing the heterogeneity of the environment, was introduced in the case of one-dimensional models in [22]. Besides addressing question (i), this allows to explore question (ii), namely possible spatial early warnings and their connection with temporal ones. The analysis of the distribution of patches, the issue (iii), is accomplished for changing values of the control parameter. The usefulness of these spatial early warnings in realistic situations and to implement remedial actions is analyzed in section 5. In section 6 we compare how these 'flags', indicating the onset of sudden shifts, display in the ecosystem under consideration and in thermodynamics. The conclusions and final comments are presented in section 7.

2. Mean-Field Description

Our starting point is the population model introduced to describe grazing systems [19] and later used in general for several ecosystems [20] and in particular for the case of the spruce budworm [23, 24]. It involves a biomass density X which evolves in time according to:

$$\frac{dX}{dt} = rX \left(1 - \frac{X}{K} \right) - \frac{cX^2}{h^2 + X^2} \quad (1)$$

where r is the intrinsic per capita growth rate, K is the carrying capacity or the number of individuals which can be supported in a given area within natural resource limits, c is the maximum consumption rate and h is a half-saturation constant *i.e.* it corresponds to the value of X such that the effective consumption is half of the maximum consumption rate. We can rewrite (1) in terms of non-dimensional quantities: $t' = rt$, $X' = X/h$, $K' = K/h$ and $c' = c/(hr)$, as

$$\frac{dX'}{dt'} = X' \left(1 - \frac{X'}{K'} \right) - c' \frac{X'^2}{1 + X'^2} \quad (2)$$

In what follows, for simplicity, we will omit the $'$ for the non-dimensional variables. The r.h.s. of (2) may be thought as the gradient of a potential V associated to the

problem:

$$V = - \int dX \left[X \left(1 - \frac{X}{K} \right) - c \frac{X^2}{1 + X^2} \right] = -\frac{X^2}{2} + \frac{X^3}{3K} + c(X - \arctan X) \quad (3)$$

so the equilibria correspond to the roots of the first derivative of V :

$$X \left(1 - \frac{X}{K} \right) - c \frac{X^2}{1 + X^2} = 0 \quad (4)$$

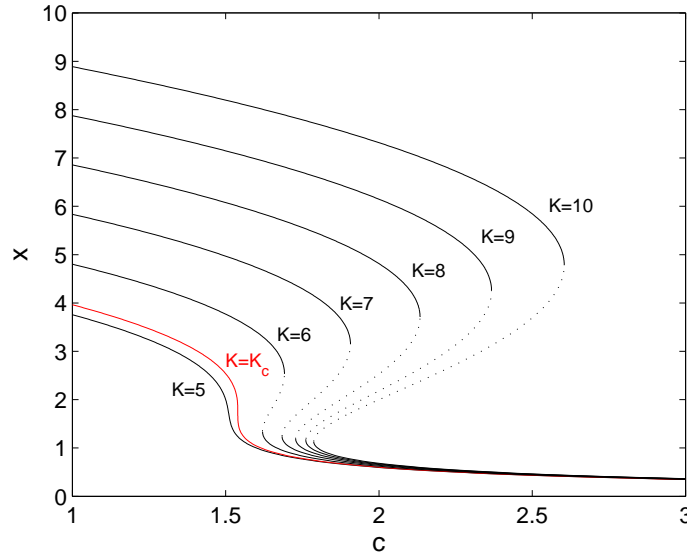


Figure 1. Folding diagrams for different values of K .

This equation has one or three real roots (besides the trivial unstable solution $X = 0$), corresponding to one stable equilibrium state or two alternative stable states (separated by an unstable one). It's interesting to notice that the presence of alternative stable states is linked to the functional form assumed for the density dependent consumption. This can be modelled by different consumption functions, which are subdivided in three classes: linear (or Holling type I), hyperbolic (or Holling type II) and sigmoidal (or Holling type III) [25]. Only for the sigmoidal consumption there occur two stable equilibria separated by an unstable one and therefore we have ASS.

In figure 1 the response curve for (4) is depicted for different values of K . For $K \leq K_c = 3^{3/2} \simeq 5.196$ only one stable solution exists for each c . As long as we consider quasi stationary evolution for increasing c , the system would exhibit a smooth response. On the other hand, for $K > K_c$, the response curve is folded backwards at two *saddle-node* bifurcation points. For certain values of c the system can be found either in the upper or the lower stable branch. For increasing c , the system starts on the upper branch and varies its state smoothly until a threshold value is found, where a catastrophic transition to the lower branch occurs. If at this

point c is decreased, we would not be able to recover the state of the system before the transition. Instead, the system would remain on the lower branch, until we decrease c enough to reach another threshold value and 'jump' to the upper branch. From an ecological management viewpoint, it would be desirable to anticipate these transitions.

A general formalism for treating these catastrophic regime shifts is the *Elementary Catastrophe Theory* (ECT) developed by R. Thom [21]. However, ECT works for static and homogeneous (MF) systems, where there is no time or spatial dependence of the potential. To discuss dynamics or local properties, ECT must be extended by incorporating some external assumptions. A change of the control parameter, reflecting changes of the external conditions, modifies the form of the potential. Therefore, as the shape of the potential changes, an original global minimum in which the system sits may become a metastable local minimum because another minimum assumes a lower value, or it even may disappear. In this case the system must jump from the original global minimum to the new one. ECT does not tell us when, and to which minimum, the jump occurs. The criterion which determines this is called a *convention*. Before discussing conventions we need to introduce two important sets of points in parameter space which control structural changes of the potential.

The first of such sets of points is the *bifurcation set* \mathcal{S}_B [26]. It divides the phase space into two regions corresponding either to single stability or bistability of the system (see figure 2). For the (c, K) points on this curve the second derivative of the potential V vanishes, so the bifurcation set is given in its parametric form by:

$$c = \frac{(x_1^2 + 1)^2}{2x_1^3}, \quad K = \frac{2x_1^3}{x_1^2 - 1} \quad \text{for } x_1 > 1 \quad (5)$$

The second set of points is called the *Maxwell set* \mathcal{S}_M [26]. On the Maxwell set the values of V at two or more stable equilibria are equal. In our case it is defined by:

$$\left(\frac{dV}{dX} \right)_{x_1, x_2} = 0 \quad (6)$$

$$V(x_1) = V(x_2), \quad (7)$$

(see the inset of V for $K = 7.5$, $c = 1.91$ in figure 2).

\mathcal{S}_B and \mathcal{S}_M are connected to two commonly applied criteria or conventions. Systems which remain in the equilibrium that they are in until it disappears are said to obey the *delay* convention. On the other hand, systems which always seek a global minimum of V are said to obey the *Maxwell* convention. Indeed these two conventions correspond to two extremes in a continuum of possibilities. Furthermore, real systems may obey either of these two conventions depending on the rate of change of the control parameters or on other external conditions. When the control parameters, and so the shape of V , change very slowly the system tends to follow the delay convention. On the contrary, when the control parameters change more quickly or when perturbations on the system are big enough, the Maxwell convention describes better the dynamics (more on this below).

3. Spatial Model

A two dimensional spatial version of the previous mean-field model is given by:

$$\frac{dX(x, y; t)}{dt} = X \left(1 - \frac{X(x, y; t)}{K(x, y)} \right) - c \frac{X(x, y; t)^2}{1 + X(x, y; t)^2} + D \nabla^2 X(x, y; t) \quad (8)$$

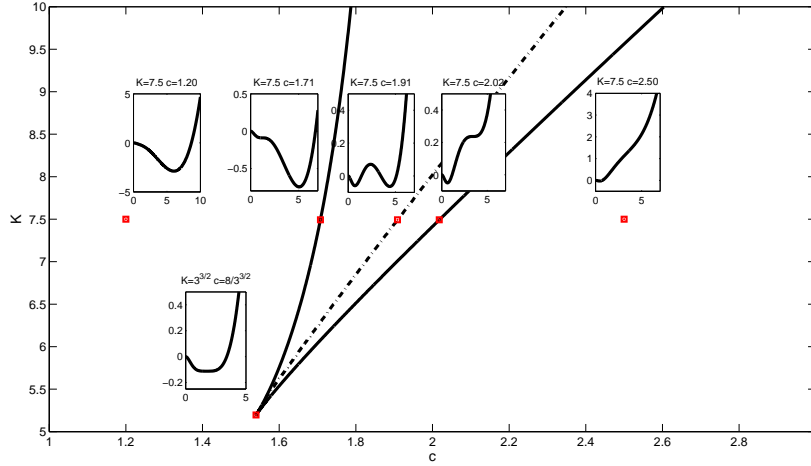


Figure 2. Bifurcation set (solid line) with a cusp point at $c = 8/3^{3/2}$, $K = K_c$ and Maxwell set (dashed). The potential V is shown for selected values of c and K .

where the carrying capacity $K(x, y)$ is a spatial heterogeneous parameter that varies from point to point (while the parameter c is taken as uniform) and D is the diffusion coefficient measuring dispersion of X in space (given in units of the intrinsic growth rate $1/r$ from section 2). We simulated this model in a $L \times L$ regular square lattice, so each cell, centred at integer coordinates (i, j) , can be associated with a patch of the ecosystem. Each cell is connected to its four nearest neighbours *i.e.* the von Neumann neighbourhood is used. To ensure numerical stability of the discretization scheme even for big values of the diffusion coefficient, the *Alternating Direction Implicit Method* [27] is used, so evolution at each time step is divided into two stages, treating implicitly one of the spatial coordinates at each:

$$\begin{aligned}
 & (1 + 2\alpha)X(i, j; t + \frac{1}{2}) - \alpha X(i + 1, j; t + \frac{1}{2}) - \alpha X(i - 1, j; t + \frac{1}{2}) = \\
 & \frac{1}{2} \left[X(i, j; t) \left(1 - \frac{X(i, j; t)}{K(i, j)} \right) - c \frac{X(i, j; t)^2}{1 + X(i, j; t)^2} \right] \\
 & + \alpha(X(i, j + 1; t) + X(i, j - 1; t)) + (1 - 2\alpha)X(i, j; t)
 \end{aligned} \tag{9}$$

$$\begin{aligned}
 & (1 + 2\alpha)X(i, j; t + 1) - \alpha X(i + 1, j; t + 1) - \alpha X(i - 1, j; t + 1) = \\
 & \frac{1}{2} \left[X(i, j; t + \frac{1}{2}) \left(1 - \frac{X(i, j; t + \frac{1}{2})}{K(i, j)} \right) - c \frac{X(i, j; t + \frac{1}{2})^2}{1 + X(i, j; t + \frac{1}{2})^2} \right] \\
 & + \alpha(X(i, j + 1; t + \frac{1}{2}) + X(i, j - 1; t + \frac{1}{2})) + (1 - 2\alpha)X(i, j; t + \frac{1}{2})
 \end{aligned} \tag{10}$$

where $\alpha = \frac{d}{8}$ and d is a reduced diffusion coefficient related with D and the lattice spacing a by $d = 4D/a^2$. Periodic boundary conditions (*PBC*) were used and L ranged from 100 to 800 (in fact, for different values of L in this range, no important differences were found). The number of time steps is typically 1000. Depending on the ecosystem, each time step could correspond to a day, or a month, or a year, etc.

The range of values for the model parameters that we use are chosen to contain the region of alternative stable states determined by the MF equations: the carrying capacity $K(i, j)$ varies randomly from cell to cell around a fixed spatial mean $\langle K \rangle = 7.5$ in the interval $[-\delta_K, \delta_K]$ where $\delta_K = 1.0 - 2.5$. Typical values for the consumption rate c are between 1 and 3 and for d are between 0.1 and 5.

3.1. Observables

Several quantities can be measured from the time series produced by the model:

- The *spatial mean* $\langle X \rangle$:

$$\langle X \rangle(t) = \frac{1}{L^2} \sum_{i,j} X(i, j, t) \quad (11)$$

(i and j locate each cell of the array).

- The *spatial variance* σ_X^2 :

$$\sigma_X^2 = \langle X^2 \rangle - \langle X \rangle^2 \quad (12)$$

- The *temporal variance* σ_t^2 computed from mean values of X at different times, $\bar{X}(t)$, (here we take $\bar{X} \equiv \langle X \rangle(t)$) which is defined as:

$$\sigma_t^2 = \frac{1}{\tau} \sum_{t'=t-\tau}^t \bar{X}(t')^2 - \left(\frac{1}{\tau} \sum_{t'=t-\tau}^t \bar{X}(t') \right)^2 \quad (13)$$

for temporal bins of size τ (typical values for τ are from 50 to 150).

- The *patchiness* or *cluster structure*. Clusters of high (low) X are defined as connected regions of cells with $X(i, j, t) > X_m$ ($X(i, j, t) < X_m$) where X_m is a threshold value. There are different criteria to define X_m , one of which is stated in section 4.
- The *two-point correlation function* for pairs of cells at (i_1, j_1) and (i_2, j_2) , separated a given distance R , which is given by:

$$G_2(R) = \langle X(i_1, j_1)X(i_2, j_2) \rangle - \langle X(i_1, j_1) \rangle \langle X(i_2, j_2) \rangle \quad (14)$$

3.2. Stable states in heterogeneous media

In this subsection we briefly describe the steady states reached by the system for static conditions, *i.e.* for constant values of the control parameter. The goal is to characterize the different alternative states, produced by eqs. (9) & (10), and their corresponding spatial patterns and to search for scaling laws.

In the absence of diffusion, each cell (i, j) would end up in an equilibrium value that is completely determined by its carrying capacity $K(i, j)$ and the initial value of X at this point. So the final state of the array would be a random distribution of values for X (see first row of figure 3). On the other hand, dispersion among cells allows for attaining global equilibrium configurations with some kind of spatial structure (second and third rows of figure 3). Notice that this structure is more noticeable as d increases.

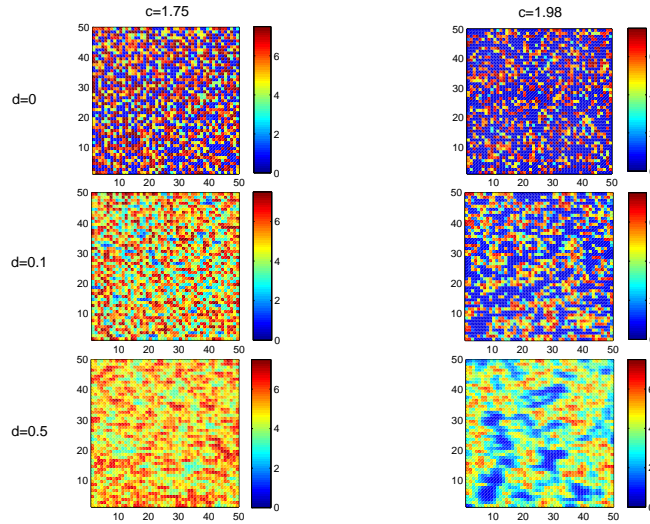


Figure 3. A portion of 50×50 cells from the original 800×800 lattice is shown, grids representing the value taken by $X(i, j)$ at each cell at equilibrium for $\langle K \rangle = 7.5$, for $c = 1.75$ (first column) and $c = 1.98$ (second column). Each row corresponds to $d = 0$, $d = 0.1$ and $d = 0.5$ respectively.

4. Alternative stable states and early warnings

Let us now study the effect of gradually increasing stress on the system, varying c from 1 to 3 in steps of $2/1000$. Therefore there is an important difference with the results presented in the previous section: now we do not let the system "thermalize", *i.e.* each measure is performed for a different value of the control parameter c .

We will see that some characteristics of the spatial structure may serve as early warnings of catastrophic shifts of the system.

4.1. Spatial and Temporal Variance

In figure 4 we compute $\langle X \rangle$, σ_X^2 and σ_t^2 in terms of increasing c with $\langle K \rangle = 7.5$, $d = 0.1$ and initial condition for each $X(i, j)$ in the interval $[0, \langle K \rangle]$. The position of peak for the spatial variance, $c_m \simeq 2.08$, is earlier than the position of peak for the temporal variance in nearly 110 time steps. So σ_X^2 works better than σ_t^2 as a warning signal for the upcoming transition. The reason for this is clear. When estimating the temporal variance one must consider past values in the time series, which correspond to situations where the ecosystem is far from undergoing a transition. The spatial variance considers only the present values, so if a signal announcing a change is present, it is not obscured by averaging it with data where these indications are not present. However, notice that when the peak in σ_X^2 occurs, $\langle X \rangle$ has already experienced a decrement of almost 50% over its initial value.

So far we have studied the shift for increasing c . Let us see what happens when c is decreased. In figure 5 the hysteresis cycles, yielded by these backward shifts, are shown for different values of d . We observe two remarkable things. First, the peak in σ_X^2 is always narrower for the backward transition than in the forward transition.

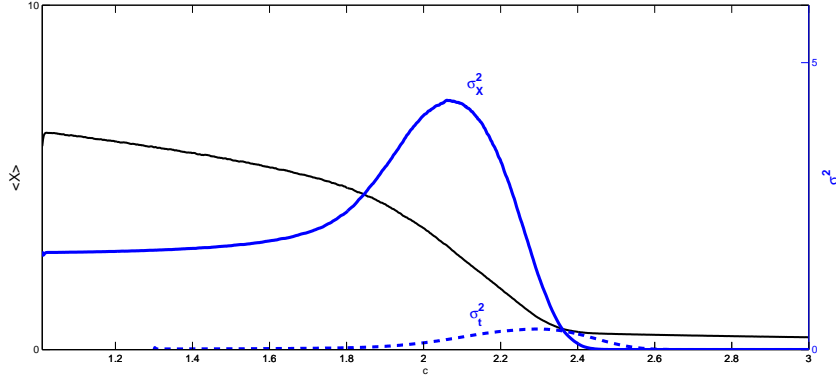


Figure 4. $\langle X \rangle$, σ_X^2 and σ_t^2 for $d = 0.1$, $\langle K \rangle = 7.5$. The peak of σ_X^2 occurs at $c_m \simeq 2.08$ and the peak of σ_t^2 at $c \simeq 2.30$.

Second, the width of the hysteresis loop decreases with d , so diffusion tends to make the transition more abrupt. We will come back to discuss the effects of diffusion in greater detail later in this section.

4.2. Correlation

The spatial variance is a particular case ($R = 0$) of the two-point correlation function (14). We wonder if considering $R \geq 1$ would give further information about a coming catastrophic shift. In figure 6 the two point correlation is depicted for $R = 0, 1, 2, 3$ (R is measured along rows or columns of the matrix array of system's cells). As one can see, the peak of the correlation for any R occurs nearly at the same value of the control parameter $c \approx c_m = 2.08$.

4.3. Patchiness: Cluster structure

In order to study the cluster structure we must define a threshold X_m as a reference for the grid values $X(i, j)$. For $\langle K \rangle = 7.5$ and $d = 0.1$ the maximum in σ_X^2 is given at $c_m \simeq 2.08$ (figure 4). The value of $\langle X \rangle$ corresponding to c_m is $\langle X \rangle_{c_m} \simeq 2.89$ and we will take it as the threshold. In the first column of figure 7 we include snapshots of typical patch configurations for $c = c_m - 0.1$, $c = c_m$ and $c = c_m + 0.1$ and in the second column a binary representation, *i.e.* dark red (blue) cells correspond to cells for which $X > \langle X \rangle_{c_m}$ ($X < \langle X \rangle_{c_m}$). The plots at the third column are the corresponding cluster distributions. At $c = c_m$ the patch-size distribution follows a power law over two decades -with exponent $\gamma \approx -1.1$ for $d = 0.1$ and $\gamma \approx -0.9$ for $d = 0.5$ - which disappears for the smaller or greater value of c . Therefore this particular distribution may be considered as a signature of an upcoming catastrophic shift in the system.

4.4. The effects of diffusion

Now we will consider the dependence on the diffusion coefficient d of the different introduced spatial signals. Figure 8 and figure 9 show, respectively, the variance and correlation for several values of d between 0 and 5.0. Notice that the influence

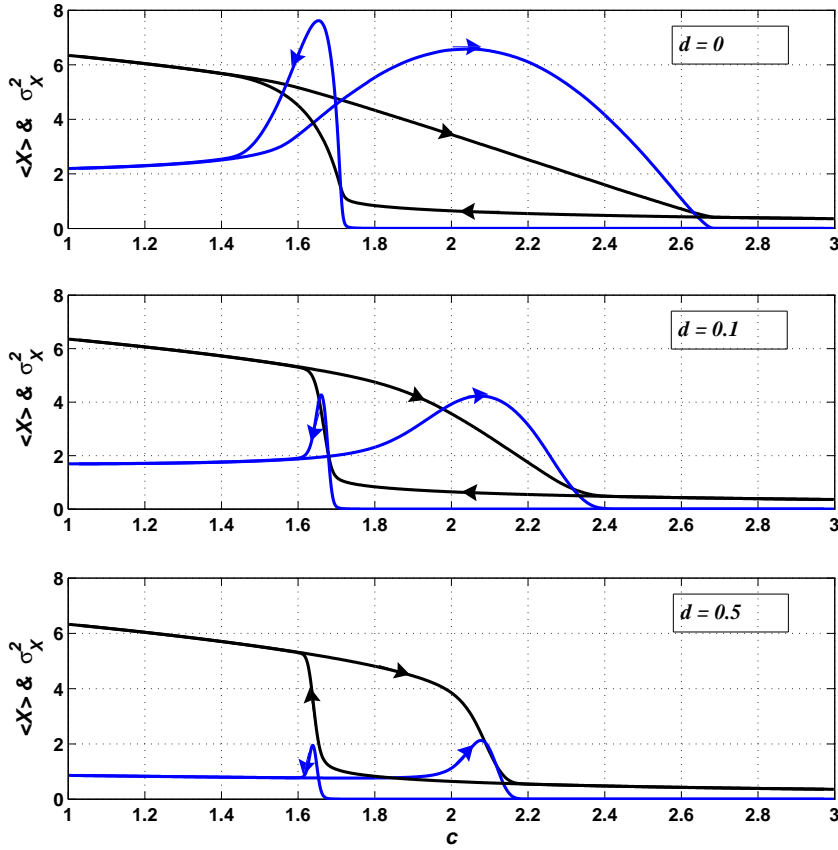


Figure 5. $\langle X \rangle$ (black curves) and σ_X^2 (blue curves) for $\langle K \rangle = 7.5$ & $\delta_K = 2.5$, computed for forward and backward changes of the control parameter c . Results for $d=0$ (above), $d=0.1$ (middle) and $d=0.5$ (below).

of diffusion on σ_X^2 and on the correlation is just the opposite. In fact for $d = 0$ there's almost no correlation and the peak of σ_X^2 is maximum. On the other hand, for $d \simeq 0.5$ the peak in the correlation is maximum whereas the peak for σ_X^2 is smaller and much more narrower. This is because we have two opposite 'forces' operating over the ecosystem. On the one hand its intrinsic underlying spatial heterogeneity ($K = K(i, j)$) promotes spatial fluctuations between nearest neighbours, while the diffusion term tends to smooth out these differences.

The resulting spatial patterns are shown in figure 10 for c_m and different values of d . For low diffusion, e.g. $d = 0.1$, a typical configuration of the system consists in small patches of arbitrary different colours (that is, large global differences, measured by the spatial variance, and low correlation). As d increases, nearest neighbour cells group into larger patches or 'supercells' of the same 'color'. The result is a lower variance and a higher correlation. For example, the values of σ_X^2 and $G_2(1)$ for $d = 0.1$ and $d = 0.5$

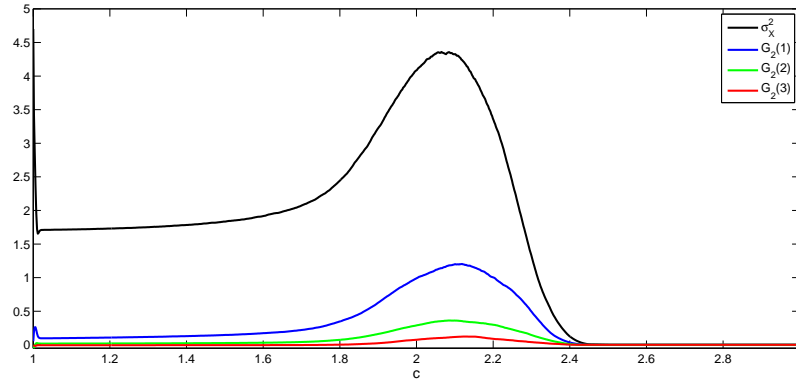


Figure 6. Two point correlation function for different lengths, $d = 0.1$, $\langle k \rangle = 7.5$.

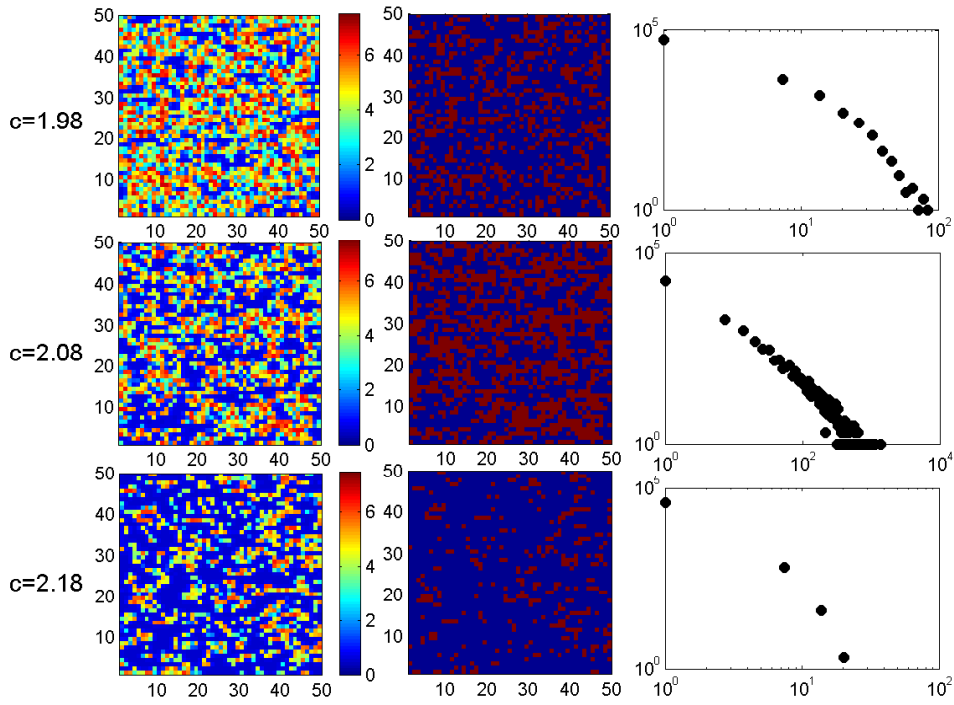


Figure 7. *First column:* A portion of 50×50 cells from the original 800×800 lattice is shown, grids representing the value taken by $X(i, j)$ at each cell for $\langle K \rangle = 7.5$, $d = 0.1$. Each row corresponds to $c = 1.98$, $c = 2.08$ and $c = 2.18$ respectively. *Second column:* same as the first for binarized data. *Third column:* Number of clusters vs. area in logarithmic scale.

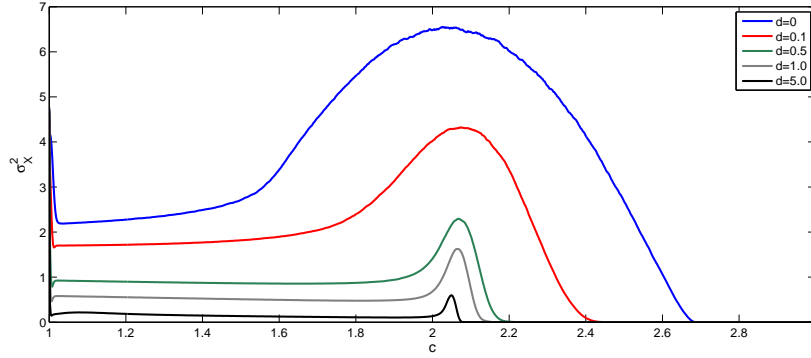


Figure 8. Spatial variance for $\langle K \rangle = 7.5$ and different values of the discrete diffusion coefficient.

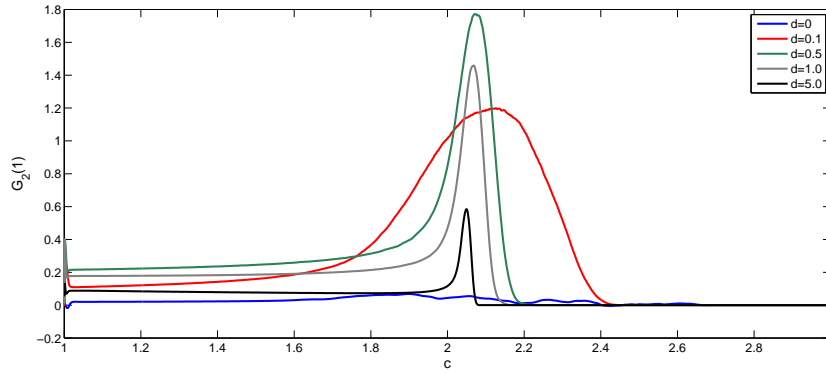


Figure 9. Two point correlation function at distance $R = 1$ for different values of the discrete diffusion coefficient, $\langle K \rangle = 7.5$.

are: $\sigma_X^2 \simeq 4.315$ for $d = 0.1$ vs. 2.292 for $d = 0.5$ and $G_2(1) \simeq 1.173$ for $d = 0.1$ vs. 1.762 for $d = 0.5$. Nevertheless if d increases even more, the color segregation is so strong that at this point the size of the supercells start to decrease lowering the correlation. So for $d = 1.0$ we have: $\sigma_X^2 \simeq 1.626$, $G_2(1) \simeq 1.458$.

5. Usefulness of the spatial early warnings

To determine the usefulness of the warning indicators presented in the previous section it is necessary 1) to assess their practicality and 2) if they really allow the implementation of corrective actions to avoid the catastrophic shift.

5.1. Practical considerations: dealing with incomplete and noisy information

Calculating variances over grids consisting in a large number of sites (e.g. 400×400 or 800×800) is easy on a computer but involves a formidable task from a measuring

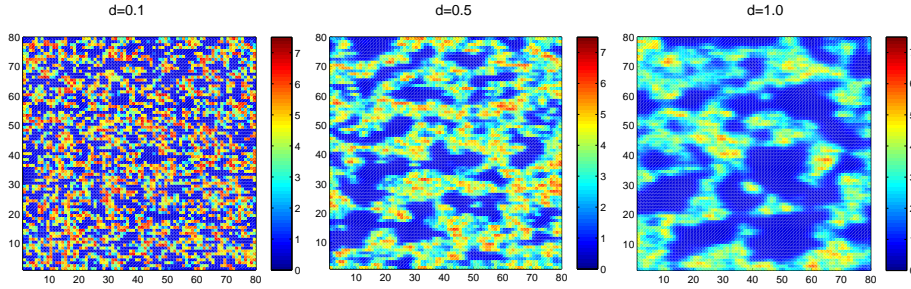


Figure 10. A coloured grid representing the value taken by $X(i, j)$ at each cell for the value of $c_m = 2.08$. A portion of the lattice containing 80×80 cells is shown. For $d=0.1$: $\sigma_X^2 \simeq 4.315$ and $G_2(1) \simeq 1.173$. For $d=0.5$: $\sigma_X^2 \simeq 2.292$ and $G_2(1) \simeq 1.762$. For $d=1.0$: $\sigma_X^2 \simeq 1.626$ and $G_2(1) \simeq 1.458$.

point of view. So, in order to assess the practical difficulty of estimating σ_X^2 , we have performed calculations over sample grids of different sizes $L_s < L$. In figure 11 we observe that the signal does not depend qualitatively on the number of points on the grid that are considered to estimate σ_X^2 . In fact, even for a very small sample of 9 points, σ_X^2 still exhibits a noticeable peak. Of course, the quality of the signal improves with the size of the sample. Additionally, since the data from real ecosystems may be very noisy, it is worth considering how the presence of noise alters results. So we assume some level of noise by adding to c a small random value belonging to some interval $[-\delta_c, \delta_c]$. In figure 12 we show $\langle X \rangle$ and σ_X^2 for $\delta_c = 0.5$. The rise of σ_X^2 and the anticipation to the temporal variance are still observed.

5.2. Possible remedial actions

We will study the consequences of a simple remedial action consisting in immediately stopping the increase of the control parameter after it reaches some threshold value c^* . In figure 13 we show the effect of keeping c constant to c^* for different values of c^* and d . For instance, if the measure is applied at the very position of the peak of σ_X^2 , $c^* = c_m \simeq 2.08$ (for $\langle K \rangle = 7.5$), its usefulness depends on the value of d . For d small ($d = 0.1$) the decay in $\langle X(t) \rangle$ stabilizes soon to a value above 2 *i.e.* the system remains in a mixed state. On the other hand, for larger values of d ($d = 0.5$) the decay in $\langle X(t) \rangle$ continues and the ecosystem passes to the alternative state with low biomass, $\langle X(t) \rangle < 1$. This figure also shows that, for $d = 0.5$, the remedial measure is effective when applied before σ_X^2 reaches its maximum at c_m , for $c^* = 1.9$. We checked that, for moderate or high diffusion ($d \gtrsim 0.5$), this recipe of management works if c^* is taken between the line corresponding to \mathcal{S}_M and the right fold line of \mathcal{S}_B (closer to the first than to the second one). So a possible criterion to choose c^* is as the points

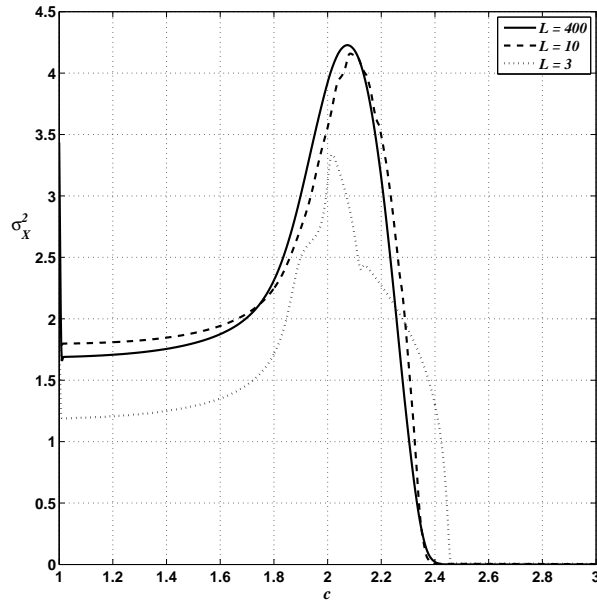


Figure 11. σ_X^2 for $d = 0.1$, $\langle K \rangle = 7.5$, $\delta_K = 2.5$ calculated on lattices of size $L_s=3$ (dotted line), $L_s=10$ and $L_s=400$ (the entire lattice).

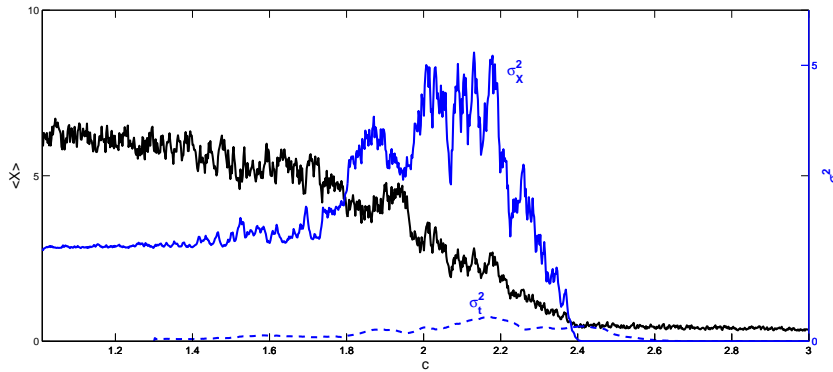


Figure 12. Same as figure 4 for $c \pm 0.5$.

belonging to \mathcal{S}_M .

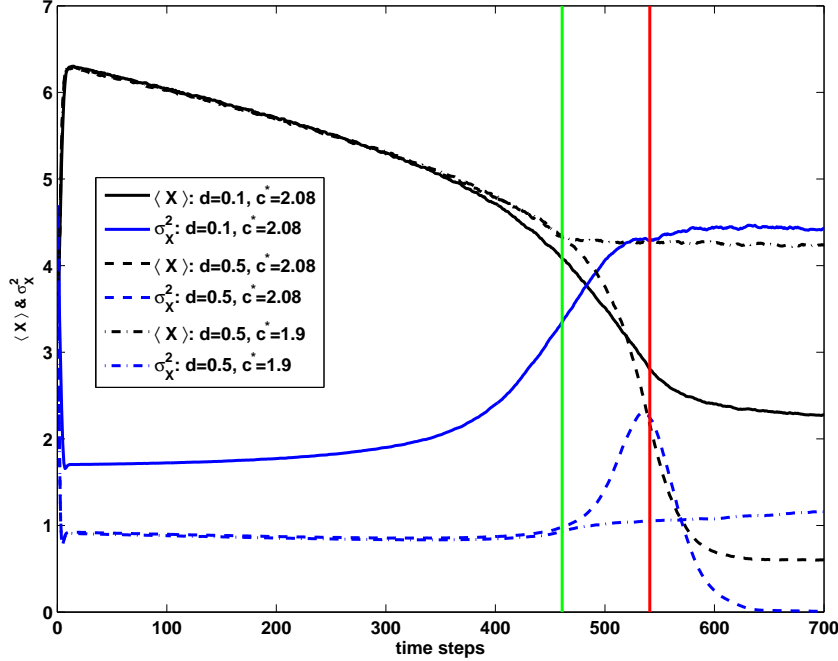


Figure 13. $\langle X \rangle$ (black) and σ_X^2 (blue) for $\langle K \rangle = 7.5$ in the case of a remedial action consisting in keeping constant the control parameter after it reaches some threshold value c^* . The red line indicates a threshold c^* coinciding with the peak of σ_X^2 , $c^* = c_m \simeq 2.08$. Full (dashed, dash-dotted) curves correspond to $d=0.1$ ($d=0.5$). The green line points a value of c^* before c_m , $c^* = 1.9$.

6. A comparison with a thermodynamic phase transition like liquid-vapour: from the delay to the Maxwell convention

Catastrophes have characteristic fingerprints or 'wave flags'. Some of the standard catastrophe flags are: *modality*, *sudden jumps*, *hysteresis* and a *large* or *anomalous variance* [26]. These are precisely the signals we found for the considered spatial heterogeneous ecological model representing a species or set of species subject to exploitation (grazing, harvesting or predation).

It is interesting to analyze similarities and differences with the liquid-vapour transition in a fluid, like water. Therefore, the biomass density X would correspond to the fluid density, the liquid to the high biomass density attractor and the vapour to the low biomass density attractor. Let us compare the above catastrophe flags for the fluid vs. the ecosystem:

- Modality: The fluid is bimodal in the neighbourhood of the liquid-gas coexistence curve, having well defined liquid and gas states. So this is similar in both systems.

- Sudden Jumps:** In the case of the fluid it is certainly true that sudden jumps occur, since there is an abrupt increase in volume when a liquid transforms into vapour. However, this large change in volume occurs when a slight change in the temperature and pressure moves the fluid from one side of the coexistence curve to the other. Hence, the liquid-vapour coexistence curve can be identified with \mathcal{S}_M and the water changes of state obey in general the Maxwell convention. On the other hand, the shift in the considered model always obeys the delay convention: the ecosystem remains in the higher attractor (higher values of X) until the bifurcation set is completely traversed. However, we have seen in section 2 that when perturbations are big enough to allow the switching between equilibria on different stability branches, the systems may follow the Maxwell convention. Hence we will consider the effect of a sudden perturbation of the environment, represented here by a sharp decrease of the average carrying capacity $\langle K \rangle$ followed by a slow recovery. Figure 14 illustrates this from a MF point of view: K is initially equal to 7.5, and for a value of the control parameter $c = 1.68$ suddenly decreases to 6. Afterwards K increases slowly in time (as c does) until it reaches its original value just before the system crosses \mathcal{S}_M at $c = 1.915$. The insets show the shape of the potential $V(X)$ just before the perturbation and after recovery.

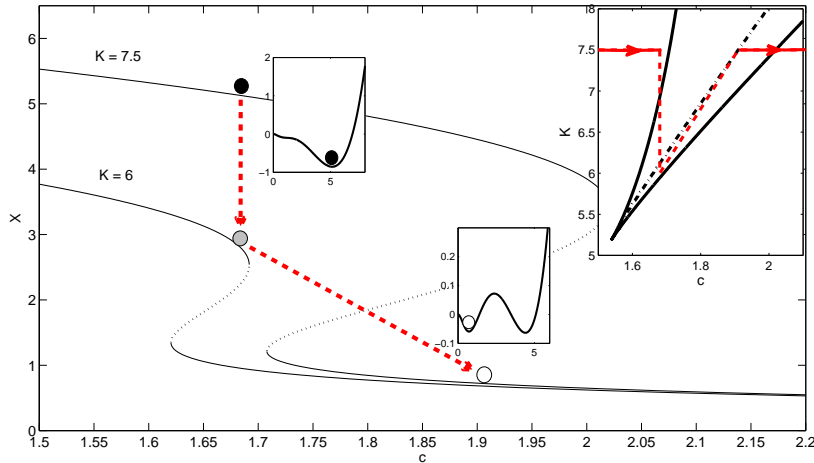


Figure 14. Variation in X produced by a global perturbation on K which suddenly decreases from 7.5 to 6 and slowly recovers later. The ecosystem is represented by a black ball before the perturbation, gray ball at intermediate step and white ball after recovery. Iso- K curves for $K = 7.5$ and 6 are depicted. The red arrow represents the perturbation. Insets show the shape of the potential $V(X)$ just before the perturbation and after recovery. *Upper right inset:* path followed by the system under perturbation in $c - K$ phase space.

What happens in the case of the spatial heterogeneous and diffusive model? In figure 15 we show the evolution of the system for a completely similar perturbation in $\langle K \rangle$. Instead of remaining close to the initial attractor (upper branch of $K = 7.5$), the system rapidly falls to the lower branch of $K = 6.0$ (which corresponds to the minimum value of the potential V). Next it approaches more

slowly to the lower branch of $K = 7.5$ until it arrives to it for $c \simeq 1.915$. So one can conclude that this type of perturbation on the system produces a change of convention: from delay to Maxwell.

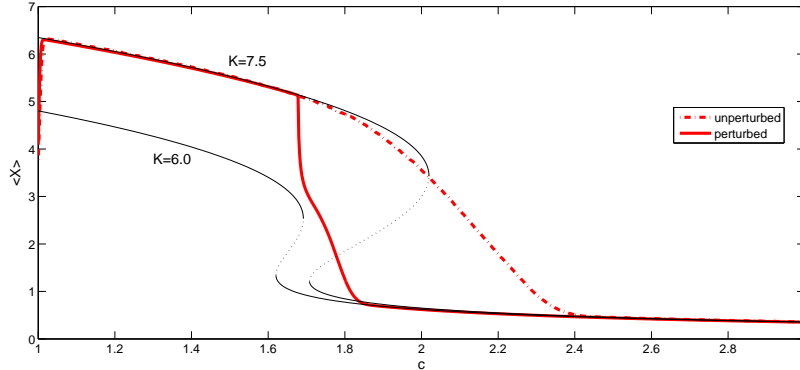


Figure 15. The effect on $\langle X \rangle$ of a global perturbation on $\langle K \rangle$ which suddenly decreases from $\langle K \rangle = 7.5$ to 6 and slowly recovers later. Thin lines represent iso- K curves for $K = 7.5$ and $K = 6.0$.

- **Hysteresis:** In everyday situations one does not observe hysteresis in the liquid-gas phase transition of water: the liquid usually boils at the same temperature at which the vapour condenses. In other words, water changes of state obey in general the Maxwell convention. Nevertheless, a careful experimentalist can obtain an hysteresis cycle by first raising the temperature and superheating the liquid, and after evaporation, cooling the gas below the condensation point. Indeed the coexistence curve is surrounded by two *spinodal lines* which determine the limits to superheating and supersaturation. These spinodal or fold lines can then be identified with \mathcal{S}_B .
- **Anomalous Variance:** When a fluid condenses (boils) from its gas (liquid) to its liquid (gas) state, small droplets (bubbles) are formed. As a consequence, the variance of the volume may become large, similarly to what happens for the ecosystem.

7. Conclusion

We have analyzed a spatial ecological model whose MF version has been widely used to describe different relevant processes, ranging from pest outbreaks to habitat desertification and harvesting of aquatic plants. This model has alternative attractors, and is subjected to random spatial dispersion.

For large enough values of the diffusion coefficient d , the system self-organizes producing characteristic spatial patterns.

When changing the control parameter c , the transition from one attractor to the other is according to the delay convention. Nevertheless, is remarkable that, the transition occurs according to the Maxwell convention when a large enough perturbation is considered. This is similar to what happens in thermodynamics. In

general we encounter the Maxwell convention in thermodynamics: water either boils or condense when it reaches the saturation temperature. However, it is possible, with sufficient care, to superheat water or supercool steam, although any disturbance will produce an immediate change of phase.

We have considered several spatial quantities both to characterize the state of the ecosystem and to use them as early warnings. Providing early warning signals is central both for management and recovery strategies of ecosystems. One of such observables is the spatial variance σ_X^2 by measuring samples of X on a grid of points. It was found that a grid containing few points might be sufficient for the purpose of extracting an appropriate signal, and that a significant growth in σ_X^2 could serve as an early warning of an imminent transition. This significant growth in the spatial variance is still observed even in the presence of moderate noise too. This is not surprising since noise, on the other hand, has been addressed as a promoting factor over persistence of alternative stable states in other ecosystems [28].

The spatial variance shows an advantage over the temporal one, as σ_X^2 soars before than σ_t^2 . The explanation for this is simple: since the former corresponds to a snapshot of the present state of the system while the latter includes in its computation data for previous times where the fluctuations were still small.

The origin of the rise in σ_X , is tied to the emergence of spatial patterns, in the form of patches of high/low concentration of X . We then conclude that the visualization of the onset of those patches, for example by aerial or satellite imaging, may be another indicator of the imminence of a catastrophic shift and an effective way of anticipating this transition. Furthermore, we found that at the very maximum of σ_X the distribution of sizes of patches becomes power law, so this particular distribution could serve as an early warning. Power law distribution has also been found in other systems as a signature of self-organization [29, 30].

Another observable of interest is the two-point correlation. We found that as long as the diffusion coefficient d increases the peak in σ_X^2 decreases and the correlation increases. This dependence on d connected to the spatial patterns that emerge as d increases is the result of two factors that point in opposite directions: the intrinsic spatial heterogeneity of the ecosystem versus the dispersion or diffusion. Therefore, for low diffusion, σ_X^2 is the most appropriate of these two indicators to detect catastrophic shifts while the correlation works less well. On the other hand, for high diffusion, the correlation may become a more useful quantity to analyze.

How helpful are all these warning signals in designing effective management protocols? Leaving aside economic considerations (which are beyond the scope of our analysis) this depends on different factors. For example, on the degree of diffusion (the size of d): The larger the diffusion the earlier the corrective action should be taken. For low values of d , a drastic measure, of immediately freezing the consumption rate c , is effective even when it has reached the value c_m at which the spatial variance is maximal. For larger values of d the remedial action taken at c_m can no longer avoid the catastrophic shift. Instead, provided there are no large perturbations, a simple quantitative criterion to take the remedial action is when c is over the line \mathcal{S}_M . We have also seen that abrupt changes of the environmental conditions, reflected as sudden large variations of the parameters, can precipitate the transition to the low biomass catastrophic alternative state. It is worth to remark that early warning signals just provide a time where it is still possible to act, but not at all when the situation is easily reversible.

Of course, the quantitative details of our conclusions depend on the choice of

parameter values employed in our model. Nevertheless, we have verified that the qualitative behaviour of our results do not depend strongly on those values. Rather it appears that our main conclusions should hold: spatial signals -variance, correlation and patchiness- are earlier than the temporal variance. Furthermore, spatial patterns formed in the process could be the fastest detectable warning that a catastrophic change is about to occur. Similar results have also been found for an eutrophication model [31] where alternative stable states are also present.

Finally, in Ecology, as far as we know, the studies focus either on spatial early warnings (for instance refs. [15, 16]) or on temporal signals (e.g. [17, 18, 32]). The link between these is novel. On the other hand, in the statistical physics of systems close to a phase transition, the connection between spatial and temporal phenomena -like hysteresis, critical slowing down, long range order, etc.- is well known. While the theory of phase transitions is well understood in thermodynamic equilibrium, its use in nonequilibrium systems is rather new. However, many of the fundamental concepts of equilibrium phase transitions - like scaling and universality- still apply in systems without a hermitian Hamiltonian but rather defined by transition rates, for which the local time-reversal symmetry is broken [33]. Moreover, in nonequilibrium systems a (dynamical) scaling of variables may occur even in first order transitions, when the order parameter jumps at the transition. This is exactly the kind of phenomenon we are observing for a spatial ecological model.

Acknowledgments

We wish to thank V. Dakos, R. Donangelo, N. Mazzeo, M. Scheffer and E. van Nes for many fruitful discussions. Work supported in part by PEDECIBA (Uruguay) and Project PDT 63-013.

References

- [1] L J McCook. Macroalgae, nutrients and phase shifts on coral reefs: scientific issues and management consequences for the great barrier reef. *Coral Reef*, 18:357–367, 1999.
- [2] M Nystrom et al. Coral reef disturbance and resilience in a human-dominated environment. *Trends Ecol. Evol.*, 15:413–417, 2000.
- [3] M Scheffer et al. Floating plant dominance as a stable state. *Proc. Natl. Acad. Sci. USA*, 100:4040–4045, 2003.
- [4] D Ludwig et al. Sustainability, stability, and resilience. *Conservation Ecology*, 1(7), 1997. <http://www.consecol.org/vol1/iss1/art7>.
- [5] B H Walker. Rangeland ecology: understanding and managing change. *Ambio*, 22:2–3, 1993.
- [6] M Scheffer. *Ecology of Shallow Lakes*. Chapman & Hall, 1998.
- [7] S R Carpenter et al. Management of eutrophication for lakes subject to potentially irreversible change. *Ecol. Appl.*, 9:751–771, 1999.
- [8] M Scheffer et al. Catastrophic shifts in ecosystems. *Nature*, 413:591–596, 2001.
- [9] S Carpenter. Alternate states of ecosystems: evidence and some implications. In Huntly N. Press, M. C. and S. Levin, editors, *Ecology: achievement and challenge*, pages 357–381. Blackwell, London, UK, 2001.
- [10] E K Steinberg and P Kareiva. Challenges and opportunities for empirical evaluation of spatial theory. In D. Tilman and P. Kareiva, editors, *Ecology: achievement and challenge*, pages 318–332. Princeton University, 1997.
- [11] S A Levin and S W Pacala. Theories of simplification and scaling of spatially distributed processes. In D. Tilman and P. Kareiva, editors, *Ecology: achievement and challenge*, pages 271–296. Princeton University, 1997.
- [12] M R Aguiar and O E Sala. Patch structure, dynamics and implications for the functioning of arid ecosystems. *Tree*, 14:273–277, 1999.

- [13] C A Klausmeier. Regular and irregular patterns in semiarid vegetation. *Science*, 284:1826–1828, 1999.
- [14] J von Hardenberg et al. Diversity of vegetation patterns and desertification. *Phys. Rev. Lett.*, 87:1981011–1981014, 2001.
- [15] M Rietkerk et al. Self-organized patchiness and catastrophic shifts in ecosystems. *Science*, 305:1926–1929, 2004.
- [16] S Kéfi et al. Spatial vegetation patterns and imminent desertification in mediterranean arid ecosystems. *Nature*, 449:213–217, 2007.
- [17] S R Carpenter and W A Brock. Rising variance: a leading indicator of ecological transition. *Ecology Letters*, 9:311–318, 2006.
- [18] W A Brock and S R Carpenter. Variance as a leading indicator of regime shift in ecosystem services. *Ecology and Society*, 11(9), 2006. <http://www.ecologyandsociety.org/vol11/iss2/art9/>.
- [19] I Noy-Meir. Stability of grazing systems: an application of predator-prey graphs. *Jour. of Ecology*, 63:459–482, 1975.
- [20] R M May. Thresholds and breakpoints in ecosystems with a multiplicity of stable states. *Nature*, 269:471–477, 1977.
- [21] R Thom. *Structural Stability and Morphogenesis*. Reading: Benjamin, 1975.
- [22] E van Nes and M Scheffer. Implications of spatial heterogeneity for catastrophic regime shifts in ecosystems. *Ecology*, 86:1797–1807, 2005.
- [23] D Ludwig, D D Jones, and C S Holling. Qualitative analysis of insect outbreak systems: the spruce budworm and forest. *Jour. Anim. Ecology*, 47:315–332, 1978.
- [24] J D Murray. *Mathematical Biology*. Springer-Verlag, 1993.
- [25] C S Holling. The components of predation as revealed by a study of small mammal predation of the european pine sawfly. *Can. Entomol.*, 91:293–320, 1959.
- [26] R Gilmore. *Catastrophe Theory for Scientists and Engineers*. Dover, 1981.
- [27] W H Press et al. *Numerical Recipes. The Art of Scientific Computing*. Cambridge University Press, third edition, 2007.
- [28] P D’Odorico, F Laio, and L Ridolfi. A probabilistic analysis of fire-induced tree-grass coexistence in savannas. *The American Naturalist*, 167:E79–E87.
- [29] M Pascual, M Roy, F Guichard, and G Flierl. Cluster size distributions: signatures of self-organization in spatial ecologies. *Phil. Trans. R. Soc. Lond. B*, 357:657–666, 2002.
- [30] J Vandermeer, I Perfecto, and S M Philpott. Clusters of ant colonies and robust criticality in a tropical agroecosystem. *Nature*, 451:457–460, 2008.
- [31] R Donangelo, H Fort, V Dakos, M Scheffer, and E H van Nes. Early warnings of catastrophic shifts in ecosystems: Comparison between spatial and temporal indicators. *Int. Jour. Bif. and Chaos*, 2009. at press.
- [32] V Dakos, M Scheffer, E H van Nes, V Brovkin, V Petoukhov, and H Held. Slowing down as an early warning signal for abrupt climate change. *Proc. Natl. Acad. Scien.*, 105:663–724, 2008.
- [33] G Ódor. Universality classes in nonequilibrium lattice systems. *Rev. Mod. Phys.*, 76:663–724, 2004.